

Ultrathin silicon nitride microring resonator for biophotonic applications at 970 nm wavelength

Cite as: Appl. Phys. Lett. **97**, 081108 (2010); <https://doi.org/10.1063/1.3483766>

Submitted: 04 June 2010 . Accepted: 08 August 2010 . Published Online: 25 August 2010

Ilya Goykhman, Boris Desiatov, and Uriel Levy



View Online



Export Citation

ARTICLES YOU MAY BE INTERESTED IN

[Propagation losses of silicon nitride waveguides in the near-infrared range](#)

Applied Physics Letters **86**, 121111 (2005); <https://doi.org/10.1063/1.1889242>

[Group velocity dispersion and self phase modulation in silicon nitride waveguides](#)

Applied Physics Letters **96**, 061101 (2010); <https://doi.org/10.1063/1.3299008>

[Effect of size and roughness on light transmission in a Si/SiO₂ waveguide: Experiments and model](#)

Applied Physics Letters **77**, 1617 (2000); <https://doi.org/10.1063/1.1308532>

Lock-in Amplifiers
up to 600 MHz



Ultrathin silicon nitride microring resonator for biophotonic applications at 970 nm wavelength

Ilya Goykhman, Boris Desiatov, and Uriel Levy^{a)}

Department of Applied Physics, The Benin School of Engineering and Computer Science, The Center for Nanoscience and Nanotechnology, The Hebrew University of Jerusalem, Jerusalem 91904, Israel

(Received 4 June 2010; accepted 8 August 2010; published online 25 August 2010)

We experimentally demonstrate a high-Q ultrathin silicon nitride microring resonator operating at wavelength of 970 nm that is favorable for large variety of biophotonic applications. Implementation of thin device layer of 200 nm allows enhanced interaction between the optical mode and environment, while still maintaining high quality factor of resonator. In addition, we show the importance of spectral window around 970 nm to improve device sensing capability. © 2010 American Institute of Physics. [doi:10.1063/1.3483766]

In recent years we are witnessing an ongoing effort for the miniaturization and integration of optical devices on chip. A key feature in reducing the dimensions of photonic devices is to use optical components based-on high refractive index contrast materials facilitating a tight confinement of light and dense integration on chip. A promising approach is to employ silicon platform for realization of miniaturized photonic components owing to its high refractive index and compatibility with standard complementary metal-oxide-semiconductor (CMOS) process. However, silicon cannot be the material of choice for applications in the visible and near infrared spectrum below 1.1 micron as it is opaque for wavelengths below the band gap. Additionally, the transmission of high power optical signals in silicon waveguides at wavelengths above the band gap can be considerably attenuated by free carriers' absorption via two photon process.¹

Among the variety of operation wavelengths, the spectral window below one micron introduces particular interest for bio-optical applications. Specifically, for *in vivo* optical trapping and sensing of biocells there is a window of relative transparency in the near infrared portion of spectrum around 750–1200 nm.² This regime is bounded by absorption of proteins toward the visible (<750 nm) and the increasing absorption of the water toward the infrared (>1200 nm). Moreover, a substantial variation with wavelength of optical damage to biological specimens is observed even within the near infrared region with damage minima occurring at 970 nm.² Consequently, for large variety of bio-optical applications it is desired to operate at the wavelengths around 970 nm. As a result we are seeking for a high refractive index optical material characterized by compatibility with standard CMOS technology and high scalability, side by side with low optical loss and low sensitivity to temperature variations for the realization of laboratory on a chip platform operating at spectral window around 970 nm.

Silicon nitride (SiN) is one of the best known candidates to fulfill the aforementioned requirements since it is transparent both in the visible and the infrared spectrum, it possess moderately high refractive index ($n \sim 2$) and being a dielectric material with large energy band gap SiN does not suffer from free carriers' absorption at wavelengths above 300

nm.^{3–5} Another advantage of SiN for biosensing applications is its low thermo-optic coefficient ($\sim 10^{-5} \text{ K}^{-1}$) making it less sensitive to environmental variations.

Along with material considerations, the integration of a resonance cavity into a bio-optical system provides an enhanced light-matter interaction, increased sensitivity and improved trapping functionality while keeping the small dimensions of the device.^{2,6–9} Specifically, the microring and microdisk resonators are widely used for this purpose^{8–12} owing to their relatively ease of design and fabrication, high quality factor and versatility in optimizing their transfer function. In this work we demonstrate an ultrathin ($\sim \lambda/5$), high-Q SiN microring resonator tailored for environmental sensing in aqueous environment and optimized to operate around the wavelength of 970 nm. Using a thin device layer facilitates strong interaction of the optical mode with the environment, while still providing decent confinement required for device miniaturization.

To realize the device we first deposited a 200 nm low-pressure chemical vapor deposition SiN layer onto 2.5 μm -thick thermally grown silicon oxide. The refractive index of the SiN layer was measured by variable angle spectroscopic ellipsometry (VASE) and found to be 2.04 at the wavelength of 970 nm. Next, both the bus waveguide and the microring resonator were defined using standard electron-beam lithography with 20 KV acceleration voltage and ZEP-520A as an electron-beam resist, following by inductively coupled reactive ion etching (ICP RIE) with a CHF_3/O_2 gas mixture. The optical structure was designed to support a TE-like mode (Transverse electric, in-plane polarization) with waveguide width and height of 850 nm and 200 nm, respectively. The waveguide dimensions were chosen as a compromise between the desire for dense integration requiring

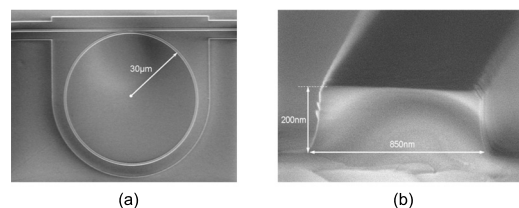


FIG. 1. (a) Scanning electron micrograph of SiN microring resonator. (b) Cross section of the SiN waveguide.

^{a)} Author to whom correspondence should be addressed. Electronic mail: ulyevy@cc.huji.ac.il.

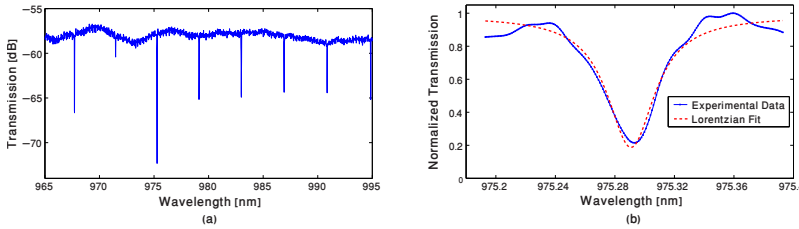


FIG. 2. (Color online) (a) Measured transmission spectrum of the device. (b) Lorentzian fit to a single resonance for obtaining the quality factor of the resonator.

high confinement of the optical mode in the waveguide core and the need for significant interaction of the light with the surrounding aqueous media. In addition, the low thickness of SiN minimizes the tensile stress within the device layer, thus providing low material loss of the waveguide.⁵

Figure 1 demonstrates the scanning electron micrograph of the fabricated structure with 30 μm ring radius and 300 nm coupling gap between the bus waveguide and the resonator. The effective refractive index of our waveguide is 1.64, as calculated by the finite element method assuming aqueous top cladding with refractive index of 1.33.

To characterize the fabricated device we performed transmission measurements using a tunable laser with spectral window of 965–995 nm (New Focus 6300), where the light was launched into the bus waveguide by a polarization maintaining tapered fiber using a butt coupling configuration. According to the experimental results presented in Fig. 2 we obtained a maximal quality factor of 75 000 and extinction ratio up to 15 dB. By fitting the measured transfer function of the device at the vicinity of different resonance wavelengths we estimated the intrinsic loss of the resonator (~ 0.033 dB/round trip) and the coupling coefficient (~ 0.032) between the bus and the ring waveguides.¹³

To appraise the environmental sensing capability of the device we repeated the transmission measurements for different concentrations of sodium chloride (NaCl) in the upper cladding aqueous solution. At 20 $^{\circ}\text{C}$ the refractive index of an aqueous solution of NaCl varies by 0.0018 refractive index units (RIU) per 1% mass.¹⁴ For small variations of the upper-cladding refractive index (Δn_c), first-order correction to the resonance wavelength can be found by:

$$\Delta\lambda = \lambda_0(\Gamma/n_{\text{eff}})\Delta n_c, \quad (1)$$

where λ_0 is the resonance wavelength of the unperturbed resonator, n_{eff} is the effective index of the waveguide, and Γ is the proportionality factor which is related to the sensitivity of the device according to $\Delta n_{\text{eff}} = \Gamma\Delta n_c$. We defined the proportionality factor Γ similarly to Refs. 15–17 and determined the sensitivity of the system using the concentration of the electric field (and not the concentration of power) in the sensing region, as follows:

$$\Gamma \equiv \frac{n_c \int_{\text{clad}} |E|^2 dA}{Z_0 \int_{\infty} |\mathbf{E} \times \mathbf{H}^*| \cdot \hat{z} dA}, \quad (2)$$

where Z_0 is the impedance of free space, \hat{z} is the unit vector along the propagation direction, and the integrals are calculated over the cross-sectional area of the waveguide. According to the measurement results presented in Fig. 3 the increasing salt concentration results in an expected red shift [Eq. (1)] in the resonance wavelength of the device.

By performing a linear fit to the experimental data [Fig. 3(b)] we estimated a maximal resonance shift of 0.164 ± 0.007 nm for 1% variation in NaCl (refractive index change of 1.8×10^{-3}) in the upper cladding solution. This value comes in reasonable agreement with the theoretical estimation of resonant wavelength shift of $\Delta\lambda = 0.172$ nm, that is calculated by Eq. (1) with an effective refractive index $n_{\text{eff}} = 1.64$. The proportionality factor was evaluated using Eq. (2) and found to be $\Gamma = 0.16$. From the slope of the fit curve [Fig. 3(b)] we found the sensitivity of the device $S = \Delta\lambda/\Delta n_c \approx 91$ nm/RIU. Our sensitivity is about two times lower compared with previous work based on SiN slot waveguides.¹⁸ Yet, the Q factor of our device is ~ 25 times higher than that of Ref. 18. The realization of high Q factor devices contributes to improved detection capability of the system due to the narrowing of the resonance linewidth,¹⁶ which in turn enables to detect smaller changes in resonance wavelength, and thus [according to Eq. (1)] allows to observe smaller variations in the refractive index of the cladding material.

To emphasize the importance of operational spectral window around the wavelength of 970 nm we found out the loss and coupling coefficients of the microring resonator¹³ in cases of air cladding (bare device) and liquid environment. Based on calculation results presented in Fig. 4 the changes in total quality factor of the device at the presence of refractive index variations in the upper cladding (with and without aqueous solution) are primarily due to the fluctuations of the coupling coefficient between the bus waveguide and the ring, while the intrinsic loss (intrinsic quality factor) of the resonator remains almost the same.

This fact shows that at operation wavelengths around 970 nm, which are preferable for large variety of biological species, one can preserve the high sensitivity required for

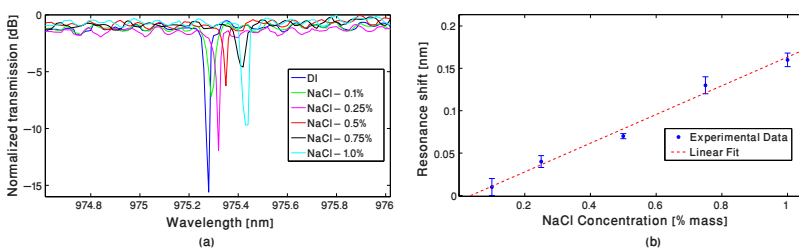


FIG. 3. (Color online) (a) Sensitivity of the device to small variations in the refractive index of upper cladding. The variation in the extinction ratio of the resonance dips is due to the limited sampling resolution in the spectral domain of the tunable laser. (b) Linear fit to the corresponding shift in resonance wavelength.

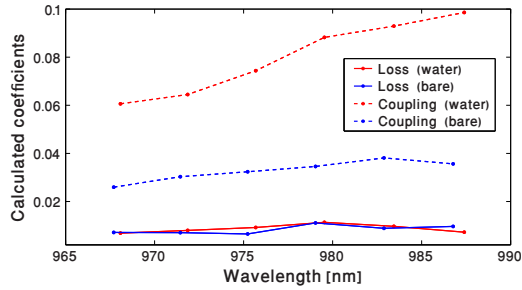


FIG. 4. (Color online) Loss and coupling coefficients of the microring resonator with air cladding (bare device) and with liquid environment, calculated from the measured data.

biosensing applications in an aqueous environment because of the negligible degradation of the optical system caused by absorption of the water at this wavelength regime. In addition, it is also possible to further improve the sensitivity of the system by increasing the total quality factor of the device using an under-coupled design of the bare resonator. In such a configuration, the introduction of an aqueous solution to the upper cladding will bring about the critical coupling condition allowing both improved extinction ratio and better Q-factor compared with the presented device.

In summary, we demonstrate an ultrathin SiN microring resonator for biophotonic applications operating at a spectral window around 970 nm. The dimensional design of the device allows reasonable sensitivity (91 nm/RIU) together with a high quality factor of 75 000 and small device dimensions (radius of 30 microns). By using different NaCl concentrations in the aqueous solution we measured a linear shift in the resonance wavelength of the device. Finally, we show that the variations in the total quality factor of the system are primarily due to changes in the coupling coefficient while the intrinsic loss of the resonator remains almost the same at the presence of the liquid clad at the wavelengths around 970 nm.

The authors I.G. and B.D. equally contributed to the work. The authors acknowledge fruitful discussions with Professor Joseph Shappir and a technical support of David Shlosberg and Noa Mazursky. The research was supported in parts by the U.S-Israel Binational Science Foundation, the Israeli Science Foundation and the Peter Brojde Center for Innovative Engineering and Computer Science. The SiN waveguides were fabricated at the Center for Nanoscience and Nanotechnology, The Hebrew University of Jerusalem.

- ¹T. Liang, L. Nunes, T. Sakamoto, K. Sasagawa, T. Kawanishi, M. Tsuchiya, G. Priem, D. Van Thourhout, P. Dumon, R. Baets, and H. Tsang, *Opt. Express* **13**, 7298 (2005).
- ²K. C. Neuman and S. M. Block, *Rev. Sci. Instrum.* **75**, 2787 (2004).
- ³K. Ikeda, R. E. Saperstein, N. Alic, and Y. Fainman, *Opt. Express* **16**, 12987 (2008).
- ⁴E. S. Hosseini, S. Yegnanarayanan, A. H. Atabaki, M. Soltani, and Ali Adibi, *Opt. Express* **18**, 2127 (2010).
- ⁵A. Gondarenko, J. S. Levy and Michal Lipson, *Opt. Express* **17**, 11366 (2009).
- ⁶S. Blair and Y. Chen, *Appl. Opt.* **40**, 570 (2001).
- ⁷S. Mandal, X. Serey, and D. Erickson, *Nano Lett.* **10**, 99 (2010).
- ⁸H. J. Yang and D. Erickson, *Lab Chip* **10**, 769 (2010).
- ⁹A. Nitkowski, L. Chen, and M. Lipson, *Opt. Express* **16**, 11930 (2008).
- ¹⁰K. De Vos, I. Bartolozzi, E. Schacht, P. Bienstman, and R. Baets, *Opt. Express* **15**, 7610 (2007).
- ¹¹C.-Y. Chao, W. Fung, and L. J. Guo, *IEEE J. Sel. Top. Quantum Electron.* **12**, 134 (2006).
- ¹²A. Yalcin, K. C. Papat, J. C. Aldridge, T. A. Desai, J. Hryniewicz, N. Chbouki, B. E. Little, O. King, V. Van, S. Chu, D. Gill, M. Anthes-Washburn, M. S. Unlu, and B. B. Goldberg, *IEEE J. Sel. Top. Quantum Electron.* **12**, 148 (2006).
- ¹³S. Xiao, M. H. Khan, H. Shen, and M. Qi, *Opt. Express* **15**, 10553 (2007).
- ¹⁴*Handbook of Chemistry and Physics*, 5th ed., edited by D. R. Lyde (CRC, London, 1975–1976), pp. 1997–1998.
- ¹⁵F. Dell’Olio and V. M. Passaro, *Opt. Express* **15**, 4977 (2007).
- ¹⁶J. T. Robinson, L. Chen, and M. Lipson, *Opt. Express* **16**, 4296 (2008).
- ¹⁷J. T. Robinson, K. Preston, O. Painter, and M. Lipson, *Opt. Express* **16**, 16659 (2008).
- ¹⁸K. B. Gylfason, C. F. Carlborg, A. Kazmierczak, F. Dortu, H. Sohlström, L. Vivien, C. A. Barrios, W. van der Wijngaart, and G. Stemme, *Opt. Express* **18**, 3226 (2010).